Available online at www.sciencedirect.com
SCIENCE DIRECT
Polymer 46 (2005) 7788–7802
polymer
www.elsevier.com/locate/polymer

Ionic actuators based on novel sulfonated ethylene vinyl alcohol copolymer membranes

Alan K. Phillips, Robert B. Moore*

Department of Polymer Science, The University of Southern Mississippi, 118 College Drive #10076, Hattiesburg, MS 39406-0001, USA

Received 22 September 2004; received in revised form 21 January 2005; accepted 16 February 2005
Available online 23 May 2005

Abstract

Sulfonated ethylene vinyl alcohol copolymers have been synthesized and artificial muscles have been produced from this new class of ionomeric membrane materials. FTIR spectroscopy confirmed the modification through introduction of peaks characteristic of ester linkages between sulfosuccinic acid and vinyl alcohol. Solid-state ^{23}Na NMR showed the ionic functionalities aggregate during membrane casting, yet small angle X-ray scattering showed that nano-phase separation between the ionic domains and matrix occurs only at elevated sulfonate content. Ionic polymer metal composites were produced through an electroless deposition of platinum generating membranes that display actuation under applied electrical stimulus. The perfluorosulfonate ionomer Nafion® has been used as a benchmark to gauge the performance of the artificial muscles produced in this study. Results showed the modified EVOH IPMC's behave similar to Nafion®, yet actuation kinetics in the new ionomer are significantly slower. Pulsed gradient spin echo NMR showed water diffusion coefficients in modified EVOH to be 1/3 those in Nafion® though the water content in the new ionomer is more than double. Slower actuation kinetics are, therefore, attributed to slower water diffusion caused by a disorganized morphology in the sulfonated ethylene vinyl alcohol.

Keywords: (Ethylene vinyl alcohol) copolymer; Ionic polymer metal composite; Artificial muscles

1. Introduction

In recent years, significant research efforts have focused on the development of synthetic materials that display biomimetic properties. One class of biomimetic materials are those which show stimuli-responsive behaviors. For example, materials have been developed that are responsive to pH, temperature, magnetic and electrical stimuli, among others [1]. The exploration of materials that respond to electrical stimulus has lead to devices that can function as actuators, specifically as artificial muscles. In early studies, researchers explored naturally occurring materials, (i.e. biopolymers), that displayed some mechanoelectric effect, such as the contraction or expansion of a gel [2]. Grodzinsky and Shoenfeld showed that collagen membranes respond to applied electrical fields producing tensile forces similar to those seen in muscle tissue [3,4]. Osada and coworkers expanded this type of research into synthetic polyelectrolyte gels, demonstrating the response of swollen gels to applied electrical stimuli [5]. These electrically driven chemomechanical systems have been proposed to function through field-induced migration of ionic species through the gel causing solvent transport and contraction or bending of the sample [2].

The reversible deswelling of a gel can be used in various applications to do mechanical work, such as an actuator [6]. In an extension of electrically responsive gels, Osada and coworkers presented a polyanionic gel coupled with a cationic surfactant that can function as an actuator, deforming in response to changes in polarity of the applied electrical field [7,8]. Polyelectrolyte gels have been shown to undergo reversible deformation under dynamic applied electrical stimulus yet require immersion in solution and in many cases actuate slowly or lack mechanical stability [6]. The slow actuation of a polyelectrolyte-based gel system can be seen in the work of Liu and Calvert with the expansion and contraction of an electrically stimulated gel taking minutes [9].

In response to the difficulties associated with polyelectrolyte gel based actuators, researchers began to explore

* Corresponding author. Tel.: +1 601 266 4480; fax: +1 601 266 5504.
E-mail address: rbmoore@usm.edu (R.B. Moore).

0032-3861/$ - see front matter © 2005 Elsevier Ltd. All rights reserved.
doi:10.1016/j.polymer.2005.02.123

ionomer membrane based (i.e. solid polymer electrolytes) systems displaying similar electromechanical motions. The systems developed have been composed of ionic polymers or ionomers in composite form with conductive metallic electrodes. The ionic-polymer metal composite, or IPMC, was first demonstrated by three groups of researchers in the early 1990s, Oguro et al. [10] and Shahinpoor [11] demonstrated actuation under electrical stimulus, whereas Sadeghipour [12] demonstrated application as sensors.

IPMC's actuate under applied electrical stimulus through a mechanism similar to that seen in electroactive polyelectrolyte gels, through electrokinetic ion migration and solvent transport [13–15]. In the water-swollen state, application of an electrical stimulus causes the mobile counterions, and associated waters of hydration, to migrate to the anode (for an ionomer containing fixed anionic groups). Enrichment of water near one membrane face generates an osmotic pressure and a strain that results in bending of the composite toward the opposite electrode. If the applied field remains on, a slow relaxation of the strain is seen as water falls down the generated concentration gradient thereby allowing relaxation of the actuator. Recent theoretical work by de Gennes showed the deformation of the composite to be composed of two forces, a charge transport by movement of the mobile counterions, and a solvent transport with initial motion of the waters of hydration and later relaxation of the concentration gradient [15].

Ionic polymer metal composites are often produced through electroless deposition of a conductive metal onto the surfaces of an ionomer membrane. State-of-the art techniques involve neutralizing the ionomer with a platinum salt, which is then chemically reduced to the metallic state using a strong reducing agent such as sodium borohydride [10]. Due to diffusion of both the reducing agent and the metal salt, selective deposition occurs at the membrane faces creating surface electrodes, which allow application of the electric potential across the membrane. The IPMC cross-section is thus composed of an ionomeric interior with metallic layers at each surface penetrating microns deep into the surface of the membrane. Advances in composite formation include multiple reductions [16], electrochemical deposition [17,18], the use of alternative reducing agents [19] and the use of other metals [18,20,21].

A review of the current open literature reveals that functional IPMC applications have focused almost exclusively on the class of perfluorosulfonated ionomers, including Nafion® from DuPont, Flemion® from Asahi Glass and Aciplex® from Asahi Chemical. Nafion® is a perfluorinated copolymer composed of tetrafluoroethylene and a perfluorovinyl ether comonomer with a sulfonic acid terminus on the side chain [22]. As a result of phase separation between the hydrophobic matrix and the hydrophilic side chains, Nafion® morphology consists of ionic aggregates distributed through a PTFE matrix. The resultant dynamic electrostatic network gives Nafion® unique mechanical and more importantly transport properties when applied in the solvent swollen state. Given the hydrophilic–hydrophobic phase separation within Nafion®, hydration occurs through swelling of the ionic aggregates [23] which can be considered roughly as reverse micellar structures distributed through the fluorocarbon matrix [24]. Hsu and Gierke suggested these swollen inverse micelles of roughly spherical geometry are connected by nano-scale hydrophilic channels concurrent with the unique transport properties exhibited by PFSI's [25]. In addition to the early work of Hsu and Gierke, numerous more recent models have been proposed for the morphology of Nafion®, ranging form lamellar models [26] to rod-like models [27]. Though the models differ significantly in the geometry proposed, each recognizes the aggregation of ionic functionalities within the matrix to be central to efficient transport through the membrane [28].

As a new alternative matrix material for IPMC systems, ethylene vinyl alcohol copolymers (EVOH) present an intriguing chemical structure composed of hydrophobic ethylene units and hydrophilic vinyl alcohol units. In the dry state, EVOH materials have found numerous applications that take advantage of their inherent gas barrier properties [29]. However, EVOH is hygroscopic and absorbs water at high relative humidity losing much of it is barrier performance [30]. Thus hydration of the hydrophilic vinyl alcohol component transforms the material from a barrier membrane to a potential transport membrane. Considering the level of hydration achievable with unmodified EVOH materials, the introduction of ionic functionalities can increase water uptake as well as open up a number of potential applications for EVOH based ionomers [31].

Marconi and coworkers showed the introduction of carboxylate functionalities significantly alters the solubility and swelling behaviors of EVOH [32]. In a similar work, sulfation of EVOH using chlorosulfonic acid was found to produce a water soluble material that is highly hygroscopic [33]. For the desired application (i.e. highly swollen actuators), the introduction of sulfonic acid functionalities must be followed by a crosslinking reaction to prevent dissolution of the membrane. Rhim and coworkers utilized sulfosuccinic acid (SSA) to accomplish a similar modification on poly(vinyl alcohol) finding that swelling decreased with increasing modification [34,35]. In this work, we extend the use of sulfosuccinic acid for the modifications of ethylene vinyl alcohol copolymers to produce membranes that are very hydrophilic yet remain insoluble in the hydrated state. The work presented here utilizes modified EVOH copolymers containing sulfonic acid functionalities as IPMC's that demonstrate dynamic actuation under applied electrical stimulus. In the series of experiments presented here we examine the relationship between chemical/morphological structure and IPMC performance demonstrating that actuation is linked closely to ionomer morphology rather than a phenomenon strictly

limited to the unique chemical and physical properties of the specific class of perfluorosulfonate ionomers.

2. Experimental

Ethylene vinyl alcohol (32 mol% ethylene F104 grade) was provided by EVAL and used as received. Sulfosuccinic acid (SSA, 70 wt% solution in water), dimethyl sulfoxide, tetraamineplatinum(II) chloride hydrate and sodium borohydride were purchased from Aldrich and used as received. EVOH was first dissolved in dimethyl sulfoxide (~7 wt%) with vigorous stirring and heat. The required amount of sulfosuccinic acid solution is then calculated on a weight percent basis and added with stirring until a homogeneous solution was produced. The membrane was then solvent cast in a polytetrafluoroethylene dish at 140 °C, and the residual organic solvent remaining after casting removed by boiling the membrane in water.

The perfluorosulfonate ionomer Nafion® (E.I. DuPont de Nemours & Co.) served as the benchmark for comparison throughout this study. The membranes used in this study were Nafion® 117 with 1100 equivalent weight, 7 mil thickness. All membranes were used in the sulfonic acid form.

2.1. Ionic content and water fraction determination

The ionic content of the sulfosuccinic acid modified EVOH was determined through a back titration procedure using phenolphthalein as an indicator. A pre-weighed sample was equilibrated in excess amount of standardized base (5 mL 0.1 M aqueous NaOH) and then back titrated using 0.1 M aqueous HCl to determine the ionic content of the polymer, expressed as ion exchange capacity (IEC). The IEC value (in mequiv/g) is calculated using the following equation:

$$\mathrm{IEC} = \frac{M_{\mathrm{i,NaOH}} - M_{\mathrm{f,NaOH}}}{W_{\mathrm{dry}}} \quad (1)$$

where $M_{\mathrm{i,NaOH}}$ is the mequiv of NaOH added to the flask prior to equilibration, $M_{\mathrm{f,NaOH}}$ is the mequiv of NaOH present following equilibration and W_{dry} is the dry mass of polymer used.

Water uptake in the membranes was determined gravimetrically using the equation shown below.

$$\mathrm{Wt\ Frac\ Water} = \frac{M_{\mathrm{hyd}} - M_{\mathrm{dry}}}{M_{\mathrm{hyd}}} \quad (2)$$

M_{hyd} and M_{dry} represent the hydrated and dry mass of the membrane, respectively. The membranes were first boiled in deionized water for 1 h, the surface patted dry and weighed and the membrane then dried overnight at 70 °C under vacuum. The dried membranes were then removed and weighed.

2.2. Fourier transform IR spectroscopy

Incorporation of sulfosuccinic acid was monitored using transmission mode FTIR spectroscopy on a Bruker Equinox 55 spectrometer set at a 2 cm^{-1} resolution. Each spectrum represents 32 coadded scans ratioed against the same number of reference scans. Thin films were solvent cast onto PTFE film and cleaned in boiling water and then dried under vacuum to remove any residual solvent, prior to analysis.

2.3. Solid state ^{23}Na NMR

Solid-state ^{23}Na NMR was conducted using a Bruker MSL-400 spectrometer operating at 105.8 MHz. Samples were first converted to the sodium form by swelling overnight in 1 M aqueous NaOH followed by cleaning in boiling deionized water to remove residual NaOH. All samples were dried under vacuum at 70 °C prior to NMR analysis. Samples were run in 7.5 mm zirconia rotors with Teflon caps and spun at 4 kHz. NaCl (crystalline solid), which has a chemical shift of 7.1 ppm relative to the standard NaCl (aqueous solution) was used as an external reference to set the frequency axis.

2.4. Pulsed gradient spin echo NMR

Pulsed gradient spin echo NMR experiments were carried out on a Varian Unity Inova 500 MHz spectrometer on samples that were hydrated by boiling in deionized water for 30 min prior to measurement. The standard Stejskal–Tanner pulse sequence [36] was used with gradient strength incremented in a non-linear fashion to maximum values of 80 G/cm for Nafion® and 60 G/cm for modified EVOH. The pulse sequence used a 9 μs 90° pulse with a recycle delay of 1 s. The gradient pulse spacing was set at 30 ms with a gradient on time of 1.5–2 ms again dependent on sample.

2.5. Wide angle X-ray diffraction/small angle X-ray scattering (WAXD/SAXS)

WAXD and SAXS experiments were performed on a Siemens XPD-700P equipped with a two-dimensional, position sensitive area detector. A sealed tube source was used to produce the Cu K_α radiation ($\lambda = 1.54$ Å) with sample-to-detector distances of 8 cm for WAXD and 49 cm for SAXS. Scattering patterns were corrected for background scattering and integrated using the GADDS™ software package. The SAXS profiles are plotted as the relative intensity, I, versus the scattering wave vector, q, where $q = (4\pi/\lambda)\sin\theta$, λ is the X-ray wavelength, and θ is 1/2 the scattering angle.

2.6. Ionic polymer metal composite formation

Ionic polymer metal composites were formed through

chemical reduction of platinum onto the membrane surface [10]. Membranes were initially prepared by roughening the surface using 400 grit sandpaper and cleaned ultrasonically in deionized water. Membranes are then immersed in 2 mg/mL aqueous tetraamineplatinum(II) chloride hydrate and allowed to equilibrate overnight. After rinsing with deionized water, the membrane was immersed in deionized water and the Pt(II) salt reduced to Pt metal using 5 wt% aqueous sodium borohydride. Addition of $NaBH_4$ was carried out in seven steps at 30 min intervals over which time the temperature was ramped from 40 to 60 °C. After completing the initial series of $NaBH_4$ additions, a final addition was performed and reduction allowed to occur for 1.5 h. The membranes were then removed and rinsed in water before immersing in 0.1 M HCl to convert the material to the acid form. The reduction process was carried out for three cycles to produce the final IPMCs used for study.

2.7. Ionic polymer metal composite characterization

IPMC structure was characterized using scanning electron microscopy (SEM) and transmission electron microscopy (TEM). SEM images were acquired using an FEI Quanta 200 operating in high vacuum mode. Images were acquired for both composite surface and freeze fractured composite cross-section. TEM images were acquired using a Zeiss EM 109-T microscope imaging composites previously sectioned through cryo-microtoming.

IPMC actuation characterization was conducted using a LabView™ based system developed in-house. Actuation signals were generated using a Function Generator VI (Labview™) and sent to and external amplifier by means of a DAQ card (National Instruments PCI-6024E). IPMC samples were stored in deionized water and removed immediately prior to testing. The IPMC was mounted between copper electrodes in a custom test fixture, which was open to the environment. Actuation of the IPMC's in all experiments was conducted in the horizontal direction (i.e. motion perpendicular to the gravitational field). Samples used for measurements were 2.5 cm in length for displacement studies, 1.5 cm in length for force analysis, 0.5 cm in width in both cases and ranged in thickness from 0.2 to 0.75 mm. Displacement measurements of the actuator under test were carried out using an Imaging Solutions Group camera (LightWise LW-1.3-R-1394) interfaced to Labview™. Image analysis was carried out using Datapoint software (Xannah Applied Science and Engineering). Actuation force measurements were conducted using a load cell from transducer techniques (GSO-10) and the supplied signal conditioning circuitry (TMO-1) with acquisition carried out in Labview™. The IPMC being tested was first clamped into the test fixture and the load cell was then advanced to a position that induced a small response from the transducer (i.e. the contact position). The load cell was then moved back, using a micrometer positioner, to zero the response prior to measurement allowing measurement of the maximum force generated at zero displacement.

3. Results and discussion

3.1. Chemical characterization of sulfonated EVOH

In Fig. 1, the results of back titrations done to determine the ionic content of the sulfosuccinic acid modified EVOH are plotted as ion exchange capacity (IEC) versus the content of SSA in the reaction feed. The IEC increases in a linear fashion as increasing amounts of sulfosuccinic acid are added to the membrane indicating successful reaction between the vinyl alcohol component of the copolymer and the carboxylic acid functionality in sulfosuccinic acid. IEC values calculated for the modified EVOH membranes follow a similar trend to those reported for sulfosuccinic acid modified poly(vinyl alcohol) and are of comparable magnitude when corrected for vinyl alcohol content within the copolymer [37]. For comparison, the IEC for 1100 equivalent weight (EW) Nafion® 117 is calculated to be 0.9 mequiv/g. From this value one can see the 20 wt% sulfosuccinic acid modified EVOH is of comparable ionic content to that of Nafion® 117.

The water uptake values for the sulfosuccinic acid modified EVOH membranes are also plotted in Fig. 1 versus the content of SSA in the reaction feed. As expected, the water content increases with the degree of sulfonation. Given the more hydrophilic nature of the EVOH matrix, relative to Nafion®, the modified EVOH has a much greater tendency to swell in water, and thus comparable water contents to Nafion® are observed at lower IEC values. It should be noted, however, that for membranes modified with SSA, above 15 wt%, the highly swollen systems become gel-like and loose their structural integrity. Therefore, since the actuation response of IPMC's is driven by the behavior of water in the membranes (see below), and the IPMC formation process requires a membrane having a reasonably high structural integrity, the following studies will be focused on the use of the 15 wt% SSA modified EVOH system in comparison to the standard Nafion® 117.

Fig. 2 shows the FTIR spectra of pure EVOH and 15 wt% sulfosuccinic acid modified EVOH. The modified polymer yields a strong peak at 1730 cm^{-1}, characteristic of the C=O stretching vibration of the carbonyl functionality introduced by the sulfosuccinic acid [34]. It must be noted that a small peak exists in the pure material at this wavenumber likely the result of residual vinyl acetate in the copolymer. A second peak at 1240 cm^{-1} can be assigned to the C–O stretch in the ester group [38]. A decrease in the intensity of the hydroxyl band at 3200 cm^{-1} relative to the alkyl band at 2900 cm^{-1} is further indication of the reaction of sulfosuccinic acid and vinyl alcohol within

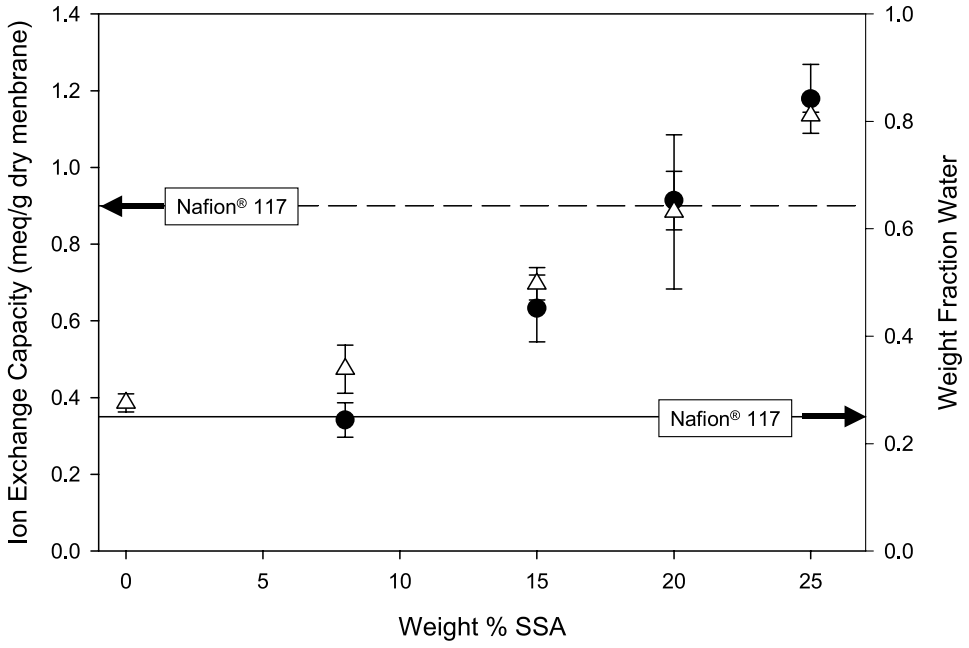

Fig. 1. Ion exchange capacity and water uptake of sulfosuccinic acid modified EVOH materials. IEC values (●) were determined through back titration and water uptake (△) determined gravimetrically. The IEC value for Nafion® 117 is denoted by the dashed line and the water uptake by the solid line.

the copolymer. The peak at 1040 cm^{-1}, which has been assigned to the symmetric stretch of the sulfonic acid functionality, also appears with sulfosuccinic acid incorporation [37].

In addition, the band at 1140 cm^{-1} disappears with sulfosuccinic acid modification. Lagaron and workers assigned this peak to ordered chain conformations within the vinyl alcohol segments of EVOH copolymers [39]. Though the all-trans chain conformations could theoretically occur anywhere within the vinyl alcohol component, the vast majority are found within the crystalline domains of the vinyl alcohol segments [40]. Therefore, disappearance of this band with sulfosuccinic acid modification suggests that chemical modification and crosslinking disrupts the crystallization of vinyl alcohol segments within the matrix.

To confirm the effect of sulfosuccinic acid incorporation on crystallinity, X-ray diffraction was used to examine the

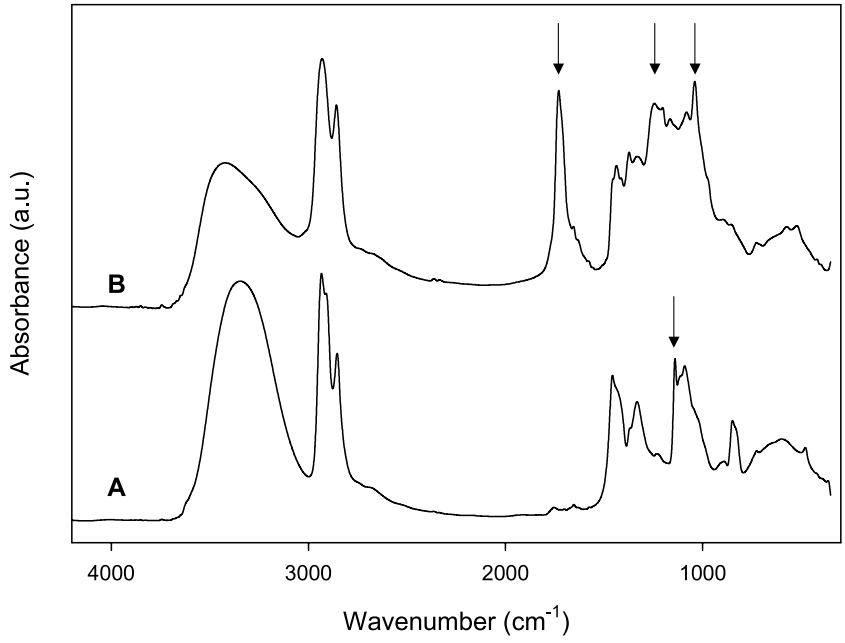

Fig. 2. FTIR spectra of pure ethylene vinyl alcohol (A) and 15 wt% sulfosuccinic acid modified ethylene vinyl alcohol (B). Data has been offset vertically for clarity.

degree of crystallinity within the samples. Fig. 3 shows the integrated diffraction profiles of pure EVOH and sulfosuccinic acid modified EVOH materials. In the pure EVOH sample, a strong peak at 20° 2θ and a smaller peak at 22° 2θ has been assigned to the 110 and 200 planes of the crystalline lattice, respectively [40]. In agreement with FTIR results, incorporation of only 1.7 wt% sulfosuccinic acid (Fig. 2(B)) results in significant loss of peak definition. These data indicate that a small fraction of modified vinyl alcohol functionalities has a significant impact on overall crystallinity. Modification at levels of 4 wt% and above results in a diffraction profile composed of only a broad amorphous halo centered around 19° 2θ.

3.2. Morphological characterization of sulfonated EVOH

Solid-state ^{23}Na NMR was used to examine the state of ionic aggregation within the matrix of sulfonated EVOH. The ^{23}Na nuclei, having a spin quantum number $I > 1/2$; possess a quadrupole moment that interacts with electric field gradients surrounding the nuclei. As a result, the nuclei are sensitive to the presence and structure of nearby ^{23}Na nuclei as well the formation of ionic complexes making ^{23}Na NMR a useful tool for studying ionic aggregation in ionomers [41]. Fig. 4 shows the solid state ^{23}Na NMR spectra of a series of sulfosuccinic acid modified EVOH materials. The spectra show two primary features, a narrow peak at 7 ppm and a broad resonance centered around −10 ppm. The narrow peak seen in the spectra has been attributed to lone sodium sulfonate ion pairs distributed throughout the matrix, while the broad resonance at −10 ppm is assigned to aggregated sodium sulfonate ion pairs [41]. Different types of aggregated sodium sulfonate ion pairs, such as dimers, trimers and larger aggregates are not resolvable thus all are represented by the broad aggregate resonance. It is of interest to note the decrease in intensity of the lone pair peak with increasing sulfosuccinic acid content indicates that, as the number of sodium sulfonate pairs introduced into the material increases, the probability of ion pairs aggregating and separating from the hydrocarbon matrix increases. However, at extremely high sulfosuccinic acid content, 63 wt%, the lone pair peak reappears. This behavior may be attributed to the high crosslink density, which lowers segmental mobility thereby 'locking' some ion pairs in an isolated state within the matrix.

Fig. 5 shows a comparison of the solid-state ^{23}Na NMR spectra of 15 wt% sulfosuccinic acid modified EVOH with that of as-received Nafion® 117. While the ionic content of the modified EVOH is slightly lower than that of Nafion®, the lone ion pair population within the modified EVOH is significantly higher and the aggregate peak is significantly broader. The increase in the lone ion pair population may be attributed to a lower driving force for aggregation; the polar vinyl alcohol content in EVOH makes the matrix far less hydrophobic than the tetrafluoroethylene matrix in Nafion® and the lower segmental mobility in the crosslinked EVOH materials tends to restrict ionic aggregation. Analysis of the aggregate resonance shows that full width at half height of the aggregate resonance in modified EVOH is ∼2.4 times that of Nafion®. The dramatic increase in peak breadth can be attributed to a number of factors that influence line shape including asymmetry of the local environment caused by nearby sodium ions and trace amounts of water as well as the distribution in the number of sodium ions within the

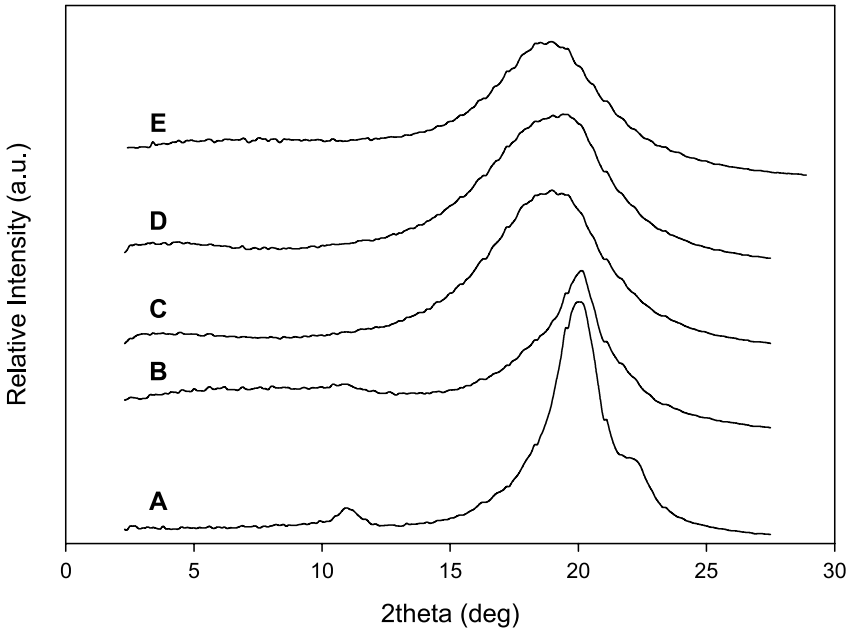

Fig. 3. Wide angle X-ray diffraction analysis of pure and sulfosuccinic acid modified ethylene vinyl alcohol. Pure EVOH (A) 1.7 wt% (B) 4 wt% (C) 8 wt% (D) and 15 wt% (E) SSA modified. Data has been offset vertically for clarity.

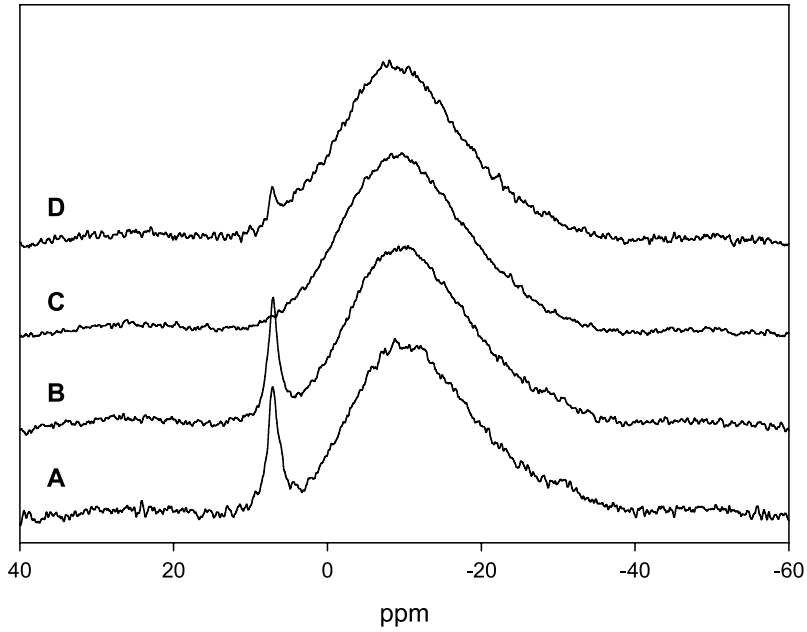

Fig. 4. Solid-state ^{23}Na NMR spectra of sulfosuccinic acid modified ethylene vinyl alcohol; 1.7 wt% (A) 15 wt% (B), 46 wt% (C) and 63 wt% (D) SSA modified. Data has been offset vertically for clarity.

aggregate [41]. Based on these factors, the increase in peak width is most likely a result of an overall symmetry within the ionic aggregates that is lower in modified EVOH than in Nafion® and a wider distribution in the number of sodium sulfonate ion pairs in the aggregates.

Small angle X-ray scattering experiments were conducted to evaluate the existence of nano-phase separated ionic domains within the membrane. SAXS studies were used to probe ionomer morphology on the nanometer scale, whereas ^{23}Na NMR confirmed ionic aggregation on the Angstrom length scale. In Fig. 6, the scattering profiles of pure and modified EVOH materials are compared to that of as-received Nafion® 117, in tetrabutylammonium form for contrast enhancement. Tetrabutylammonium neutralized Nafion® shows a strong scattering peak at a scattering wave vector, q, of 1.8 nm^{-1}, corresponding to a Bragg spacing of approximately 3.5 nm. This scattering peak, termed the ionomer peak, has been attributed to interparticle interference characteristic of the spatial distribution of aggregates within the matrix. In contrast, pure EVOH shows

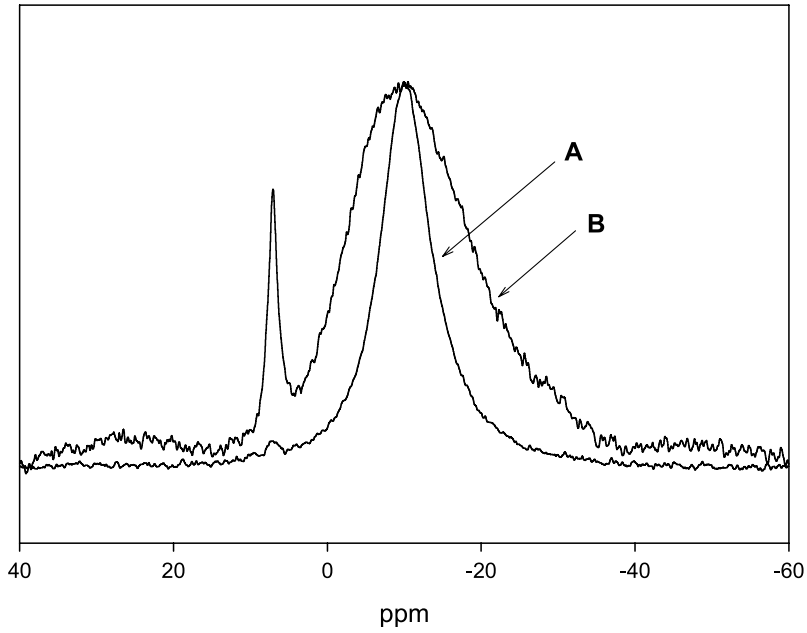

Fig. 5. Solid-state ^{23}Na NMR spectra of s received Nafion® 117 (A) and 15 wt% sulfosuccinic acid modified ethylene vinyl alcohol (B).

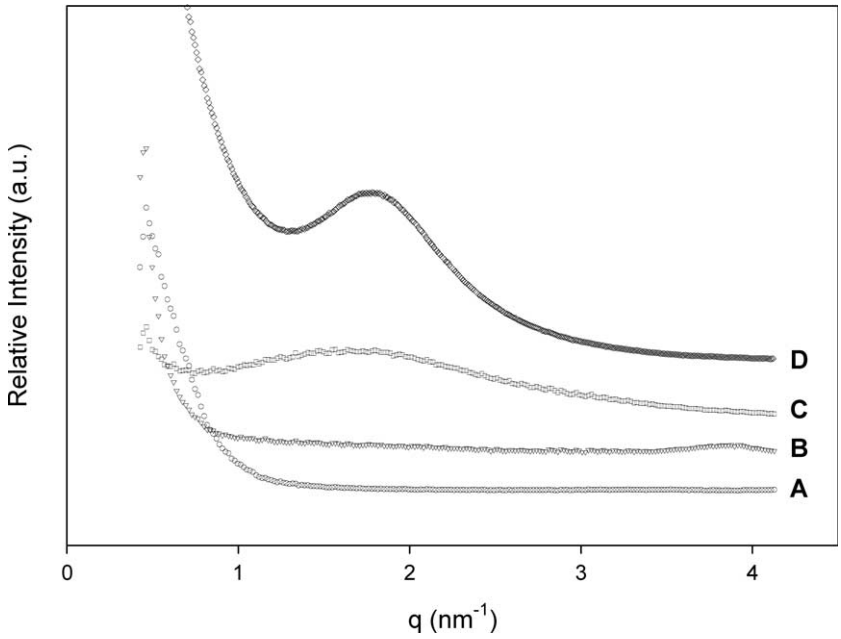

Fig. 6. Small angle X-ray scattering from ethylene vinyl alcohol (A) 15 wt% (B) and 63 wt% (C) sulfosuccinic acid modified EVOH. Tetrabutylammonium neutralized Nafion® 117 (D) is included for comparison. Data has been offset vertically for clarity.

no scattering maxima in this small angle region, indicating there are no correlations in heterogeneity on this size scale. Incorporation of 15 wt% sulfosuccinic acid also shows no ionomer peak indicating nano-phase separated ionic domains are not present within the sample. This result shows the ionic aggregates, confirmed by ^{23}Na NMR, lack a well-organized structure on the nanometer scale, such as that seen in the ionic domains of Nafion®. However, increasing the sulfosuccinic acid content to 63 wt% leads to the appearance of a very broad scattering maximum centered at 1.7 nm^{-1}, corresponding to an average separation of 3.7 nm. The low intensity and breadth of this scattering peak indicates that the ionic domains, though present in high SSA content EVOH, are far less defined than that seen in Nafion®.

3.3. Characterization of IPMC structure

Having compared the ionomer morphology of both modified EVOH and Nafion®, it is now of interest to explore the structure of IPMC's produced from each ionomer. Scanning electron microscopy (SEM) and transmission electron microscopy (TEM) were used to examine the overall structure of the IPMC as well as the structure and distribution of platinum particles within the matrix. SEM analysis of the IPMC surface, the top images in Fig. 7, shows surface layers of deposited platinum that have cracked as a result of drying the samples. In both Nafion® and sulfosuccinic acid modified EVOH, the surface appears fully covered. Lower magnification micrographs show the 'mud-cracked' texture of the Nafion® IPMC to be visible in modified EVOH, though on a larger size scale, indicating both IPMC's possess a surface layer of deposited platinum. In the case of the Nafion® IPMC, the surface appearance agrees with that shown by Shahinpoor and Kim for a composite with a surface layer of platinum deposited above an initial layer of metal just below the membrane surface [42]. The lower set of images in Fig. 7 shows cross-sections of freeze fractured IPMC samples. It should be noted that the IPMC's are not shown at equal magnification due to differences in membrane thickness. Both micrographs show a thin layer of platinum deposited on each membrane surface.

TEM analysis of microtomed samples enables analysis of the particle morphology and distribution of platinum within the IPMC. In Fig. 8, the micrographs of both Nafion® and EVOH based IPMC's show a dense layer of platinum particles at the film edge with particle density decreasing toward the film interior. The layer of dense platinum particles in each IPMC is shown to extend 2–4 μm into the membrane from the edge noted in the image. The micrographs show essentially spherical platinum particles ~50 nm in diameter agreeing well with those shown in literature [42]. The average particle size appears to be slightly larger for the case of modified EVOH IPMC's, though the overall particle density appears to be higher in Nafion® based IPMC's. The high particle density in Nafion® may be reflective of the efficiency of the ionic aggregates in nucleating particle growth. Similar reports in literature confirm the use of ionic aggregates as templates for both metallic particles [43] and other inorganics such as silicates [44]. In contrast, the lower particle density seen in the modified EVOH IPMC may result from the higher number of lone

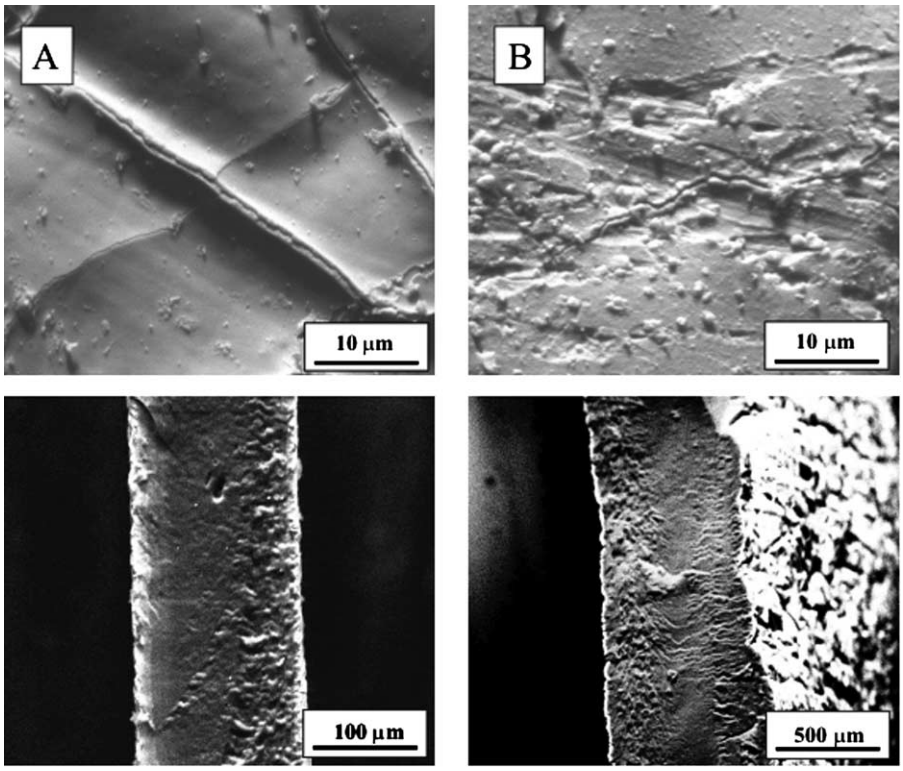

Fig. 7. Scanning electron micrographs of the surface (top) and cross-section (bottom) of Nafion® 117 (A) and 15 wt% sulfosuccinic acid modified EVOH (B) IPMC's.

ion pairs seen in ^{23}Na NMR as these lone pairs are not as effective in nucleating platinum particles. Given that similar ionic contents result in similar Pt salt uptake, larger particle size in EVOH IPMC's may result from lower nucleation density, nucleating a smaller number of particles that ultimately grow to larger size.

3.4. Ionic polymer metal composite performance

Actuation performance of the sulfocsuccinic acid modified EVOH membranes was characterized through video analysis and force measurements. Fig. 9 shows a series of images of a 15 wt% sulfosuccinic acid modified

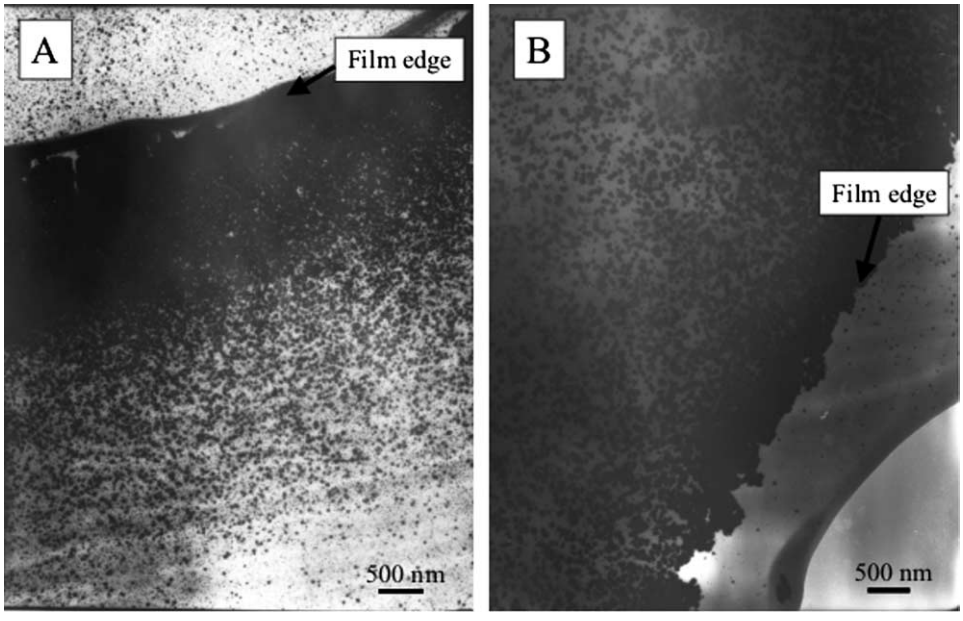

Fig. 8. TEM micrographs of Nafion® 117 (A) and 15 wt% sulfosuccinic acid modified EVOH (B) IPMC's.

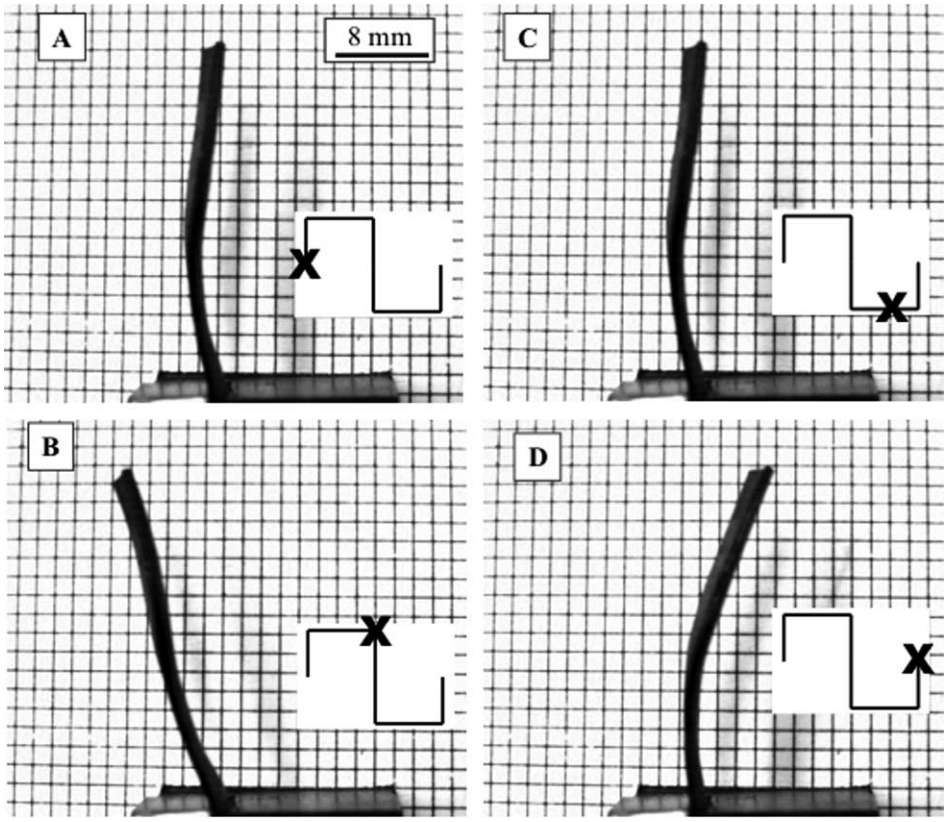

Fig. 9. Actuation in a 15 wt% sulfosuccinic acid modified EVOH IPMC. Actuator (2.75 cm length) is driven by 0.1 Hz square wave at 8 V. Inset shows the position on the excitation signal corresponding to the time of image acquisition. Image A was taken at time 0, image B at 5 s, image C at 8.5 s and image D at 10 s.

EVOH IPMC undergoing deformation in response to an 8 V, 0.1 Hz square wave. Overlaid in each image is a schema showing the position on the excitation wave, denoted by an X, at which the image was acquired. In the initial image, Fig. 9(A), the IPMC is clamped vertically between copper electrodes prior to application of the electrical stimulus. Fig. 9(B) shows the IPMC 5 s after application of the potential, immediately prior to the polarity switch of the applied square wave. The IPMC has undergone a 15° deflection from the vertical (tip displacement of ~10 mm) as mobile ions and waters of hydration migrate in response to the 8 V potential. Fig. 9(C) shows the return to the initial position as the IPMC responds to the applied voltage and bends toward the opposite electrode following the polarity switch of the stimulus, which has caused the mobile species to migrate in the opposite direction. In the final image, Fig. 9(D), the maximum deflection in the direction opposite that in Fig. 9(B) results from the polarity switch by the applied potential. Again the sample has undergone a 12° deflection from its vertical position in response to the electrical stimulus.

In Fig. 10, a comparison of the normalized tip displacement of Nafion® 117 and 15 wt% sulfosuccinic acid modified EVOH IPMC's is plotted as function of applied field strength. Normalized voltage, a measure of field strength, is necessitated by the difference in film thickness of Nafion® and EVOH IPMC's. In agreement with literature, the data shows that normalized tip displacement (displacement divided by actuator length) increases as the electrical driving force increases [45]. Deflection in EVOH based IPMC's is shown to be an approximately linear function of field strength. However, Nafion® IPMC's display a non-linear dependence on field strength with displacement scaling roughly with the square of field strength. Shahinpoor and coworkers showed a similar non-linear relationship in Nafion® IPMC's with displacement reaching saturation at higher voltages [45,46]. It must be noted in the work of Shahinpoor, displacement is characterized at drive voltages up to 7 V yet in the current study application of voltage above 3 V results in significant electrolysis as evidenced by gas production and degradation of both actuation performance and the IPMC itself.

Fig. 11 shows the actuation force produced by Nafion® 117 and 15 wt% SSA modified EVOH IPMC's as measured using the load cell system described above. Actuation forces follow the trend seen in displacement with EVOH based IPMC's showing a linear dependence on field strength and Nafion® IPMC's a non-linear dependence. However, the force in Nafion® IPMC's does not scale as strongly as that seen in displacement, scaling as field strength to the 1.8 power. At high field strength, 12 V/mm and above, the Nafion® and EVOH-based IPMC's generate forces similar

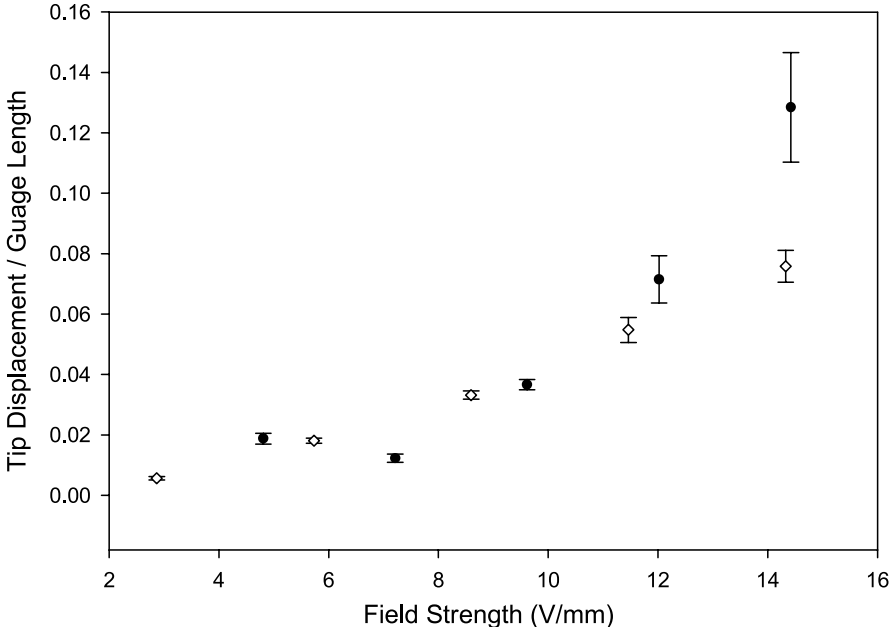

Fig. 10. Normalized tip displacement as a function of normalized voltage for Nafion® 117 (●) and 15 wt% sulfosuccinic acid modified EVOH (◇) IPMC's. Excitation signal was a 0.1 Hz square wave.

to those reported for H^+-form Nafion® based actuators [45]. As with displacement, the actuation forces are comparable over the range of evaluated field strengths.

Analyses of the actuation force results are further extended to an examination of the shape profile of the load cell response. The response profiles provide information on the development of actuation force over the course of the excitation cycle. Fig. 12 shows the load cell response of Nafion® 117 and 15 wt% SSA modified EVOH excited by a 0.1 Hz square wave. In Fig. 12(A), Nafion® based IPMC's develop maximum force at various times on the response curve as a function of electrical stimulus. At low field strength, the Nafion® IPMC achieves maximum force early in the excitation wave followed by a decay with time, indicative of the fast initial motion and slow relaxation reported in IPMC's [10,47]. However, at an intermediate field strength of 9.4 V/mm, the actuator reaches a plateau in force that does not decay, suggesting no strain relaxation.

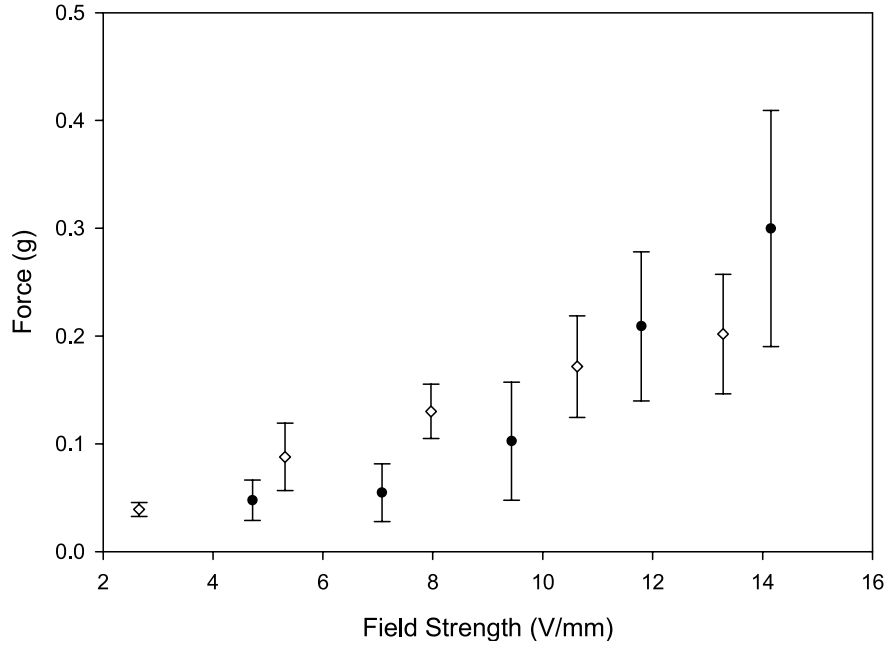

Fig. 11. Actuation forces produced by Nafion® 117 (●) and 15 wt% sulfosuccinic acid modified EVOH (◇) IPMC's. Excitation signal was a 0.1 Hz square wave.

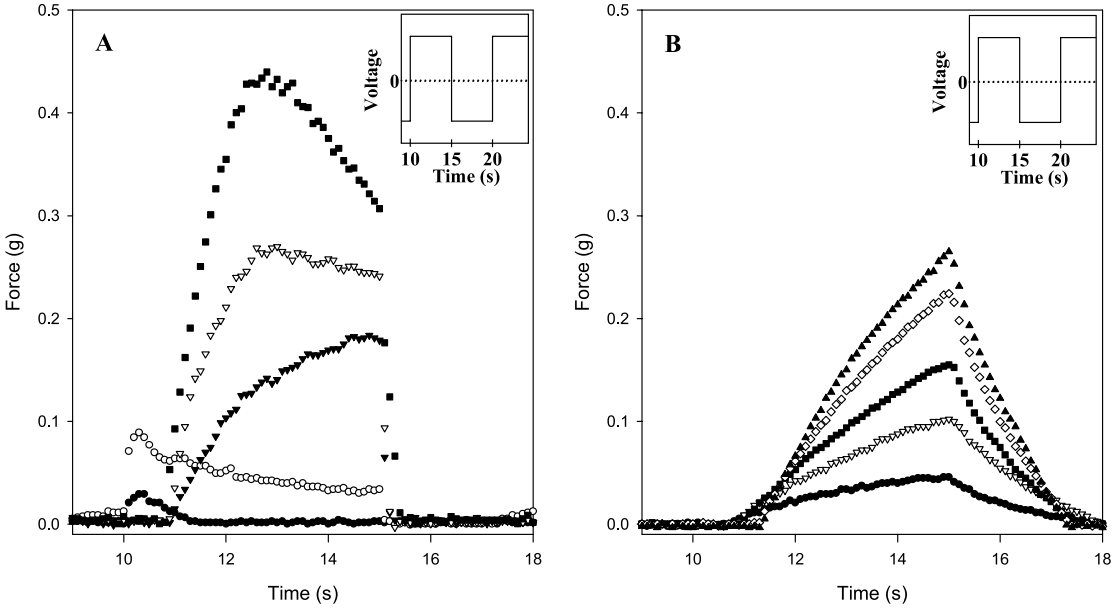

Fig. 12. Load cell responses from Nafion® 117 IPMC (A) and 15 wt% sulfosuccinic acid modified EVOH IPMC (B). Field strengths in A are 4.7 V/mm (●), 7.1 V/mm (○), 9.4 V/mm (▼), 11.8 V/mm (▽) and 14.2 V/mm (■). Field strengths in B are 2.7 V/mm (●), 5.3 V/mm (▽), 8.0 V/mm (■), 10.6 V/mm (◇) and 13.3 V/mm (▲). Actuators are being driven by a square wave excitation signal at 0.1 Hz with the second wavelength of the signal shown. Overlay represents excitation wave used for testing.

The initial rapid movement and subsequent slow relaxation returns at high field strengths though the maximum force is generated at a later time in the excitation cycle. In the case of all field strengths for the Nafion® IPMC's, rapid movement off the load cell is seen at the polarity switch of the excitation, occurring at 15 s in the plots shown.

For EVOH-based IPMC's (Fig. 12(B)), the force builds with time until the polarity of the field switches and then undergoes a slow deformation in the opposite direction. In contrast to the behavior of the Nafion® IPMC, the response profile remains consistent with field strength and only the magnitude of the force increases. The response curves show no evidence of rapid initial motion or strain relaxation as the actuation force builds in a near linear fashion throughout the excitation cycle. Maximum forces are achieved at 15 s immediately prior to the switch in polarity of the excitation signal. The differences in the shape of the load cell responses between Nafion® and EVOH-based IPMC's will be explored below in the context of the rate of water diffusion through the matrix.

Fig. 13 shows the tip displacement track of a Nafion® 117 IPMC actuating in response to a 0.1 Hz square wave at 2.5 V (11.8 V/mm) and an EVOH-based IPMC at 8 V (10.6 V/mm). In the displacement track of the Nafion® IPMC, a rapid initial displacement to ~70% of it is maximum displacement is followed by continued slow movement until the excitation signal switches polarity. This displacement profile agrees with the load cell response seen in Fig. 12(A), where the Nafion® IPMC (at 2.5 V excitation) builds force rapidly then slows at longer time. In the case of both the load cell response and the IPMC tip displacement track, the switch in polarity of the excitation signal is followed by a rapid motion in the opposite direction similar to that seen in the initial movement.

EVOH-based IPMC's behave significantly different in that no rapid motion is seen in either the load cell response (Fig. 12(B)) or the displacement track (Fig. 13). In both experiments, the actuator moves in a linear fashion with both force and displacement increasing through the excitation wave cycle. Following the polarity flip of the excitation signal, the EVOH-based IPMC shows a slow movement in the opposite direction, again in a linear fashion. It is of interest to note the similarity between initial slope and slope following the polarity switch seen in EVOH based IPMC's, whereas Nafion® moves much more rapidly following the polarity switch than it does initially.

Tip velocity for the IPMC's was calculated from the slope of the displacement curve in both the initial region and the region following the polarity switch [48]. These results show the Nafion® IPMC to be moving at over five times the speed of the EVOH-based IPMC during its initial fast motion and approximately eight times the speed following the polarity switch. The tip velocity in EVOH IPMC's differs by only 25% from initial to following the polarity switch, whereas in Nafion®, the velocity after the switch in excitation polarity is double the initial velocity. The tip displacement profile of modified EVOH IPMC is similar in shape to those reported by Nemat-Nasser and Wu for Nafion® IPMC's neutralized with large alkylammonium counterions [47]. In these studies, it was demonstrated that the use of large alkylammonium counterions, tetrabutylammonium specifically, slowed the rate of displacement under

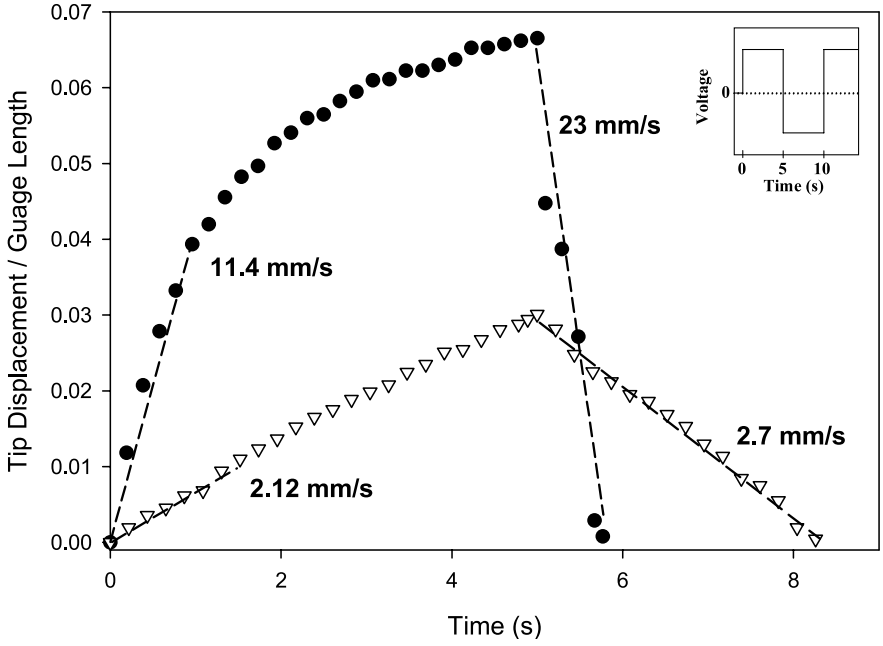

Fig. 13. Tip displacement track of Nafion® 117 (●) and 15 wt% sulfosuccinic acid modified EVOH (▽) IPMC's. Actuation at 0.1 Hz square wave signal with 2.5 V amplitude for Nafion® and 8 V amplitude for EVOH–SSA. Overlay represents excitation wave used for testing.

applied DC stimulus. The rate of diffusion of the bulky counterion was determined to cause the slow actuation, reinforcing the correlation between diffusion and actuation.

The contrasting behaviors of the two types of IPMC's investigated are likely to result from differences in water diffusion through the respective polymer matrices. Pulsed gradient spin echo NMR was used to examine the diffusion of water in the materials under study. Using gradient NMR pulses, PGSE NMR provides a noninvasive technique for studying the diffusion of species either through solution or in this case through a polymer matrix. Application of a gradient pulse allows measurement of diffusion based on attenuation of the spin-echo signal during a diffusion time within the pulse sequence. Fig. 14 shows the attenuation profiles used to calculate the diffusion coefficients using the equation below [49]

$$\ln\left[\frac{A(g)}{A(0)}\right] = -\gamma^2 D g^2 \delta^2 \left(\Delta - \frac{\delta}{3}\right) \tag{3}$$

Plotting the natural log of the ratio of signal intensity with gradient strength g, $A(g)$, and the intensity with no gradient, $A(0)$, versus the square of the gradient strength g allows calculation of the diffusion coefficient D. Table 1 shows the calculated diffusion coefficients for both Nafion® 117 and 15 wt% sulfosuccinic acid modified EVOH in addition to the water content of each sample. The PGSE NMR experiments reveal that the water diffusion coefficient in 15 wt% EVOH–SSA is approximately 1/3 that measured for Nafion®, although sulfosuccinic acid modified EVOH contains a higher water content. This result suggests that the percolation pathway for water in sulfosuccinic acid modified EVOH is more tortuous than in Nafion®. This observation is in agreement with SAXS analysis which shows that modified EVOH lacks the well organized, nano-phase separated ionic domains seen in Nafion®. As a result, slower diffusion through the disorganized morphology causes the EVOH based IPMC to respond slower than Nafion®.

Table 1
Diffusion coefficients for Nafion® and 15 wt% sulfosuccinic acid modified EVOH measured through pulsed gradient NMR experiments and the water content of each measured gravimetrically

Sample	D ($\times 10^6$ cm^2/s)	λ (moles H_2O/mole SO_3^-)
Nafion 117	6.07	20
15 wt% SSA modified EVOH	2.17	55

4. Conclusions

In this paper the formation of a novel cross-linked and sulfonated ethylene vinyl alcohol copolymer is described. Characterization of the sulfosuccinic acid modified EVOH ionomer shows that EVOH can be successfully modified using sulfosuccinic acid and the incorporated sulfonic acid functionalities aggregate during membrane casting. However, at intermediate SSA incorporation (15 wt%) the EVOH ionomer lacks an ionomer peak in SAXS suggesting that distinct nano-phase separation between ionic domains and matrix in sulfonated EVOH does not exist.

Using a series of neutralization and chemical reduction cycles, the modified membranes are converted to ionic

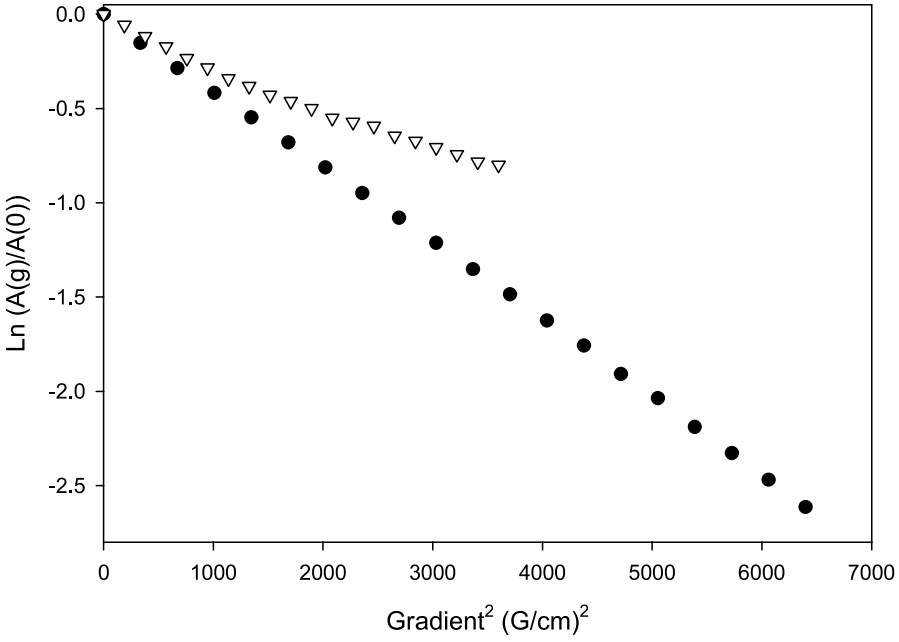

Fig. 14. Signal attenuation plot used in pulsed gradient NMR experiments to measure the diffusion of water through the matrix. Nafion® (●) and 15 wt% sulfosuccinic acid modified EVOH (▽).

polymer metal composites that demonstrate actuation under applied electrical stimulus. The ionomer morphology of each material apparently has a significant effect on the nucleation and growth of platinum particles. With Nafion®, the distinct ionic clusters are likely to be more effective at nucleating particle growth, relative to the less organized ionic distribution in the sulfonated EVOH.

In comparison to the benchmark IPMC material, Nafion®, the new class of ionomers perform comparably in both displacement and force generated, although their response-time characteristics differ significantly. Actuation in modified EVOH IPMC's reveals the stimuli responsive character documented for perfluorinated ionomers is not specific to the chemical structure of these materials but to the more general ionomer morphology [50]. Linear dependences of both tip displacement and actuation force on field strength in EVOH based IPMC's differ notably from the non-linear behavior seen in Nafion®. The new class of IPMC's behave similar to literature reports of Nafion® materials which have been treated with large counterions so as to slow diffusion and actuation [47]. The actuation kinetics of modified EVOH-based IPMC's are significantly slower than that of Nafion® which has been attributed to the slow diffusion of water through the disorganized ionomer morphology present in the sulfonated EVOH matrix.

Acknowledgements

This work was supported primarily by the MSREC Program of the National Science Foundation under Award Number DMR0213883. The authors also acknowledge Dr William Jarrett for assistance with both ^{23}Na and PGSE NMR.

References

[1] Bar-Cohen Y. EAP History, Current Status and Infrastructure. In: Bar-Cohen Y. Electroactive polymer [EAP] actuators as artificial muscles. Bellingham, WA: SPIE; 2001. p. 3–44.
[2] Osada Y, Gong J. Prog Polym Sci 1993;18:187–226.
[3] Grodzinsky AJ, Shoenfeld NA. Polymer 1977;18:435–43.
[4] Shoenfeld NA, Grodzinsky AJ. Biopolymers 1980;19:241–62.
[5] Kishi R, Osada Y. J Chem Soc, Faraday Trans I 1989;85:655–62.
[6] Calvert P. Electroactive Polymer Gels. In: Bar-Cohen Y. Electroactive polymer [EAP] actuators as artificial muscles. Bellingham, WA: SPIE; 2001. p. 123–38.
[7] Osada Y, Okuzaki H, Hori H. Nature 1992;355:242–4.
[8] Okuzaki H, Osada Y. Polym Gels Networks 1994;2:267–77.
[9] Liu Z, Calvert P. Adv Mater 2000;12:288–91.
[10] Asaka K, Oguro K, Nishimura Y, Mizuhata M, Takenaka H. Polym J 1995;27:436–40.
[11] Shahinpoor M. Smart Mater Struct 1992;1:91–4.
[12] Sadeghipour K, Salomom R, Neogi S. Smart Mater Struct 1992;1:172–9.
[13] Asaka K, Oguro K. J Electroanal Chem 2000;480:186–98.
[14] Nemat-Nasser S, Li JY. J Appl Phys 2000;87:3321–31.
[15] de Gennes PG, Okumura K, Shahinpoor M, Kim KJ. Europhys Lett 2000;50:513–8.
[16] Pak JJ, Cha S-E, Ahn H-J, Lee S-K. 32nd International symposium on Robotics: Seoul, Korea. vol. 3 2001. p. 1980–1984.
[17] Shahinpoor M, Kim KJ. Smart Mater Struct 2000;9:543–51.
[18] Tamagawa H, Nogata F, Watanabe T, Abe A, Yagasaki K, Jin J-Y. J Mater Sci 2003;38:1039–44.
[19] Kim KJ, Shahinpoor M. Smart Mater Struct 2003;12:65–79.
[20] Onishi K, Sewa S, Asaka K, Fujiwara N, Oguro K. Electrochim Acta 2000;46:737–43.
[21] Bennett MD, Leo DJ. Smart Mater Struct 2003;12:424–36.

[22] Eisenberg A, Kim JS. Introduction to ionomers. 1st ed. New York: Wiley; 1998.
[23] Gebel G, Aldebert P, Pineri M. Polymer 1993;34:333–9.
[24] Gierke TD, Munn GE, Wilson FC. J Polym Sci: Polym Phys Ed 1981; 19:1687–704.
[25] Hsu WY, Gierke TD. J Membr Sci 1983;13:307–26.
[26] Litt MH. Polym Prepr 1997;38:80–1.
[27] Rubatat L, Rollet A-L, Gebel G, Diat O. Macromolecules 2002;35: 4050–5.
[28] Mauritz KA, Moore RB. Chem Rev 2004;104:4535–96.
[29] Lagaron JM, Powell AK, Bonner G. Polym Test 2001;20:569–77.
[30] Zhang Z, Britt IJ, Tung MA. J Polym Sci Part B: Polym Phys 1999;37: 691–9.
[31] Phillips A, Domenech A, Wolbert M, Moore RB. Polym Prepr 2004; 45:535–6.
[32] Marconi W, Piozzi A, Marcone R. Eur Polym J 2001;37:1021–5.
[33] Marconi W, Marcone R, Piozzi A. Macromol Chem Phys 2000;201: 715–21.
[34] Rhim J-W, Yeom C-K, Kim S-W. J Appl Polym Sci 1998;68: 1717–23.
[35] Rhim J-W, Park HB, Lee C-S, Jun J-H, Kim DS, Lee YM. J Membr Sci 2004;238:143–51.
[36] Stejskal EO, Tanner JE. J Chem Phys 1965;42:288–92.
[37] Kim DS, Park HB, Rhim J-W, Lee YM. J Membr Sci 2004;240:37–48.
[38] Silverstein RM, Webster FX. Spectrometric identification of organic compounds. 6th ed. New York: Wiley; 1998.
[39] Lagaron JM, Gimenez E, Catala R, Gavara R. Macromol Chem Phys 2003;204:704–13.
[40] Lopez-Rubio A, Lagaron JM, Gimenez E, Cava D, Hernandez-Munoz P, Yamamoto T, et al. Macromolecules 2003;36:9467–76.
[41] O'Connell EM, Root TW, Cooper SL. Macromolecules 1994;27: 5803–10.
[42] Shahinpoor M, Kim KJ. Smart Mater Struct 2001;10:819–33.
[43] Mattera VDJ, Barnes DM, Chaudhuri SN, Risen WMJ, Gonzalez RD. J Phys Chem 1986;90:4819–24.
[44] Deng Q, Cable KM, Moore RB, Mauritz KA. J Polym Sci Part B: Polym Phys 1996;34:1947.
[45] Shahinpoor M, Bar-Cohen Y, Simpson JO, Smith J. Smart Mater Struct 1998;7:R15–R30.
[46] Bar-Cohen Y, Xue T, Shahinpoor M, Simpson JO, Smith J. SPIE 5th annual international symposium on smart structures and materials. San Diego, CA: SPIE; 1998. p. 6.
[47] Nemat-Nasser S, Wu Y. J Appl Phys 2003;93:5255–67.
[48] Onishi K, Sewa S, Asaka K, Fujiwara N, Oguro K. Electrochim Acta 2001;46:1233–41.
[49] Zawodzinski TA, Neeman M, Sillerud LO, Gottesfeld S. J Phys Chem 1991;95:6040–4.
[50] Akle BJ, Hickner M, Leo DJ, McGrath JE. ASME international mechanical engineering conference and exposition. Washington, DC: ASME; 2003 [paper IMECE2003-43561].